VERSITA

CELLULAR & MOLECULAR BIOLOGY LETTERS
http://www.cmbl.org.pl

Received: 11 June 2011
Final form accepted: 23 November 2011
Published online: 02 December 2011

Volume 17 (2012) pp 49-61
DOI: 10.2478/s11658-011-0036-6

Research article

THE CYTOTOXIC EFFECT OF DIPHTHERIA TOXIN ON THE ACTIN CYTOSKELETON

BAŞAK VAROL, MUHAMMET BEKTAŞ*, RÜSTEM NURTEN and ENGIN BERMEK
İstanbul University, İstanbul Faculty of Medicine, Department of Biophysics, 34390 Çapa-İstanbul-Türkiye

Abstract: Diphtheria toxin (DT) and its N-terminal fragment A (FA) catalyse the transfer of the ADP-ribose moiety of nicotinamide adenine dinucleotide (NAD) into a covalent linkage with eukaryotic elongation factor 2 (eEF2). DT-induced cytotoxicity is versatile, and it includes DNA cleavage and the depolymerisation of actin filaments. The inhibition of the ADP-ribosyltransferase (ADPrT) activity of FA did not affect the deoxyribonuclease activity of FA or its interaction with actin. The toxin entry rate into cells (HUVEC) was determined by measuring the ADP-ribosyltransferase activity. DT uptake was nearly 80% after 30 min. The efficiency was determined as $K_m = 2.2$ nM; $V_{max} = 0.25$ pmol.min^{-1}. The nuclease activity was tested with hyperchromicity experiments, and it was concluded that G-actin has an inhibitory effect on DT nuclease activity. In thepresence of DT and mutant of diphtheria toxin (CRM197), F-actin depolymerisation was determined with gel filtration, WB and fluorescence techniques. In the presence of DT and CRM197, 60-65% F-actin depolymerisation was observed. An *in vitro* FA-actin interaction and F-actin depolymerisation were reported in our previous paper. The present study thus confirms the depolymerisation of actin cytoskeleton *in vivo*.

Key words: ADP-ribosylation, Diphtheria toxin, Eukaryotic elongation factor-2, F-actin, Fragment A

* Author for correspondence. E-mail: muhbektas@hotmail.com, fax: 00 90 212 4142187

Abbreviations used: DT – diphtheria toxin; FA – fragment A; F-actin – filamentous actin; G-actin – globular actin monomer; HUVEC – human umbilical vein endothelial cells

INTRODUCTION

Diphtheria toxin (DT) is a well-characterised bacterial toxin, both in terms of its structure and its mode of action [1]. DT consists of a 535 amino acid polypeptide and contains the following three domains: the amino terminal fragment A (catalytic C domain), the carboxy terminal receptor-binding R domain, and the translocation (or transmembrane) T domain that exists between fragment A and the R domain. Fragment A (FA) is connected to the T domain both by a readily reducible disulfide bridge and an arginine-rich loop that is easily nicked by proteases [2]. CRM197 is the product of a single missense mutation (Gly^{52} to Glu) within the FA region of DT [3]. The mutation leads to an enzymatically inactive product, yielding a non-toxic mutant of DT [4]. FA is an ADP-ribosyltransferase (ADPrT) [5] that catalyses the transfer of an ADP-ribosyl group of NAD to a post-translationally modified histidine (diphthamide) residue on eukaryotic elongation factor 2 (eEF2) [6]. The entry of the FA into the cytoplasm is requisite for the cytotoxic action of DT [7]. After the R domain of DT binds to a DT receptor (DTR) on the cell surface, DT is internalised by receptor-mediated endocytosis [8, 9]. When DT changes its conformation in an acidic compartment, certain regions of the T domain are inserted into the endosomal membrane. Finally, the enzymatically active FA is translocated to the cytosol [10]. As a result of this process, eukaryotic protein synthesis inhibition occurs. DT-induced degradation of actin filaments may also deserve consideration because the toxin is known to cause severe, often lethal cardiomyopathy associated with diphtheria (diphtheria myocarditis) [11]. Another aspect of DT-induced cytotoxicity is the depolymerisation of actin filaments following the inhibition of protein synthesis. Moreover, actin has been recently shown to inhibit FA-mediated ADP-ribosylation of eEF2 [12]; this finding indicates the necessity to determine the nature of the interactions between these proteins. DT-FA can interact with both G- and F-actin. The binding to the latter appears to take place at the plus end of the filament, blocking further polymerisation [13]. Moreover, the role of F-actin and eEF2 in the endocytic trafficking of DT was determined in our findings [14]. The present study investigates the effect of HUVEC FA on the actin cytoskeleton. Furthermore, to elucidate the cytotoxic effect, the rate of toxin entry into cells and the nuclease activity of DT were determined through *in vitro* and *in vivo* experiments.

MATERIALS AND METHODS

Materials

All reagent grade biochemicals were purchased from Sigma (St. Louis, MO, USA). [adenosine-^{14}C]NAD^+, specific activity 535 Ci/mol, was purchased from Perkin Elmer Life Sciences (Waltham, MA, USA), and the anti-FA monoclonal antibody (mouse) [7F2] was purchased from Abcam (UK). DT was a gift of the

Refik Saydam Institute in Ankara, and it was additionally obtained from Calbiochem (USA). Botulinum C2 toxin was from Sigma. G-actin/F-actin in vivo assay kit BK037 was from Cytoskeleton, Inc. (USA). The activity of FA was determined with an ADP-ribosylation assay. The reaction was carried out for 10 min at 20°C in 20 μl reaction mixtures containing 50 mM Tris-HCl, pH 7.4, 7 mM ME, 2 μM [^{14}C]NAD and 20 μg/ml of FA [15]. Rat liver eEF2 was prepared as described [16].

Treatment of cells with DT

Human umbilical vein endothelial cells (HUVEC-ATCC ECV 304) propagated in DMEM-F12 containing 10% fetal calf serum were distributed in 35 mm diameter culture wells (10^6 cells/well) with 0.8 μM of DT in the medium. After the indicated periods of time, the cells were harvested using a cell scraper (Greiner Bio-One) and washed three times in phosphate buffered saline (PBS). They were homogenised in 1% (v/v) Nonidet P-40, 150 mM NaCl, 50 mM Tris-HCl, pH 7.5, in the presence of protease inhibitors (Complete Tablets, Roche Applied Science).

Deoxyribonuclease assay

The deoxyribonuclease assay was carried out essentially as described in [17]. Stock solutions of DNase I (Boehringer Mannheim) were prepared at 10 mg/ml, and 50-100 μg of calf thymus DNA (Boehringer Mannheim) was digested in a 0.5 ml reaction volume. In the control experiment, the amount of DNase I that yielded an 80% increase in A260 measurements in 20 min at 20°C was determined. The reaction buffer contained 50 mM Tris-HCl, pH 7.5, 0.5 mM ATP, 0.5 mM $CaCl_2$, 10 mM NaCl, 3 mM $MgCl_2$, 0.01 mM phenylmethylsulfonyl fluoride, and the indicated amounts of DNase I or FA. The inhibition of deoxyribonuclease activity was determined.

Gel filtration analysis

The size distributions were analysed on a Sepharose 4B column (1 x 60 cm). The column was in turn equilibrated and run with F-actin buffer [13], and it was calibrated using ribonuclease (M_r 13.7 kDa), G-actin (M_r 42.5 kDa), bovine serum albumin (BSA) (M_r 67 kDa), β-galactosidase (M_r 116 kDa), and ferritin (M_r 450 kDa). The reaction volume was 1 ml. The amount of material in fractions was quantified by absorption measurements at 280 nm. Actin amounts were determined by ELISA.

Enzyme-linked immunosorbent assay (ELISA)

The assay method for ELISA reported by Engvall was essentially followed [18]. A total of 100 μl of each sample was added (actin and fragment A) to the wells of plates. The wells were then incubated with an antibody buffer (PBS containing 1% bovine serum albumin and 0.1% Tween-20) at 37°C for 30 min to block non-specific binding sites. The wells were then incubated in parallel with an anti-actin antibody (Santa Cruz) and anti-fragment A (7F2) (diluted 1/1000 in

the antibody buffer) for 2 h at 37°C. After washing with PBS, bound antibody was detected using a secondary horseradish peroxidase-conjugated anti-mouse IgG antibody (1/1000 in antibody buffer) for 1 h at 37°C. After a final wash in PBS, the peroxidase activity was detected in line with the instructions as specified by the Abbott OPD (O-phenylenediamine dihydrochloride) reagent kit (Bio-Rad). The amounts of actin and fragment A were determined by measuring the absorbance at 490 nm (A490) with increasing amounts of standards of these two proteins.

Western blotting

SDS-PAGE was performed as described [19]. β-galactosidase (*Mr* 116 kDa), phosphorylase b (*Mr* 97 kDa), conalbumin (*Mr* 75 kDa), ovalbumin (*Mr* 45 kDa), carbonic anhydrase (*Mr* 29 kDa), and ribonuclease (*Mr* 13.7 kDa) were used as molecular standards. The proteins were stained with Coomassie blue and destained in 7% acetic acid and 30% methanol. For visualisation of the protein bands corresponding to actin, the proteins separated by SDS-PAGE were transferred to nitrocellulose (Millipore) membranes that had been treated with TBS (Tris-buffered saline)-Tween (TBST) and 0.5% BSA for 1 h. The membranes were incubated with an actin-specific antibody (rabbit) and then with horseradish peroxidase conjugates of anti-rabbit IgG antibody (goat). After three washes with TBST, the substrate solution containing 3-amino-9-ethyl carbonate (Bio-Rad Laboratories, CA, USA) was added. After developing, the membranes were washed with water.

Fluorescence microscopy

Immunofluorescence microscopy was used to determine the F-actin organisation in primary cell culture articular HUVEC cells that were either left untreated or treated with DT. Briefly, primary culture cells were fixed with 3.5% paraformaldehyde in PBS for 10 min at room temperature. The cells were permeabilised and blocked in PBS containing 0.1% Triton X-100 and 5% fetal calf serum for 30 min. The actin filaments were visualised using rhodamine-phalloidin or were labelled with Alexa 497 (Invitrogen Molecular Probes, OR, USA), and the nuclei were visualised using 4',6-diamidino-2-phenylindole (DAPI) (Invitro Molecular Probes, OR, USA). The FA was detected using the murine monoclonal antibody 7F2 and fluorescein isothiocyanate (FITC)-labelled goat anti-mouse IgG antibody (Sigma). All images were obtained on an Olympus BX51 microscope equipped with a DP72 camera and controlled by the Olympus DP2-TWAIN software.

Measurement of filamentous actin (F-actin) in cells

Populations of actin filaments in cells were separated by differential centrifugation [20]. Cells were lysed in 10 mM MOPS, pH 7.0, 1% Triton-X-100, 10% glycerol, 0.5 mM EDTA, 10 mM sodium pyrophosphate, 50 mM sodium fluoride, 1 mM sodium orthovanadate, 1 mM dithiothreitol, and protease inhibitors (1 μM phenylmethanesulfonyl fluoride, 30 μg/ml aprotinin, 20 μg/ml

leupeptin, 0.5 mg/ml diisopropyl fluorophosphate, and 0.2 mg/ml *trans*-epoxysuccinyl-L-leucylamido (guanidino) butane). The lysates were centrifuged at 16,000 x *g* for 2 min. The pellet fraction contained Triton-insoluble cytoskeleton fibres (P1). The supernatant fraction was centrifuged at 100,000 x *g* for 20 min. The second pellet fraction contained Triton-soluble filamentous actin (P2), whereas the supernatant fraction (S2) contained soluble G-actin. The actin levels were determined by ELISA and G-actin/F-actin in vivo assay kit [21]. Alternatively, the amount of actin filament was measured. After toxin treatment, cells were stained with 175 ng/ml rhodamine-labelled phalloidin. Fluorescence was measured with a spectrometer (Perkin Elmer-LS 45) at excitation 544 nm and emission 590 nm [22].

Statistical analysis

Statistical analysis was performed using the unpaired Student's t-test. All results were expressed as the mean ± S.D. A $p < 0.05$ was regarded as statistically significant.

RESULTS

Cellular interactions of FA

The ADP-ribosylation of eEF2 by FA revealed that FA activity was inhibited in a time-dependent manner; after 12 h of incubation, FA activity had dropped from its original level by nearly 80% (Fig. 1). In the first experiment, nearly 75% and 95% of DT initially present in the culture medium was internalised after 30 min and 6 h of incubation, respectively (Fig. 2A). This internalisation gave rise to intracellular FA concentrations in the range of 2-5 μM. Thus, DT uptake by the cells was highly efficient (K_m = 2.2 nM; V_{max} = 0.25 pmol.min^{-1}) (Fig. 2B) and quantitative under the incubation conditions.

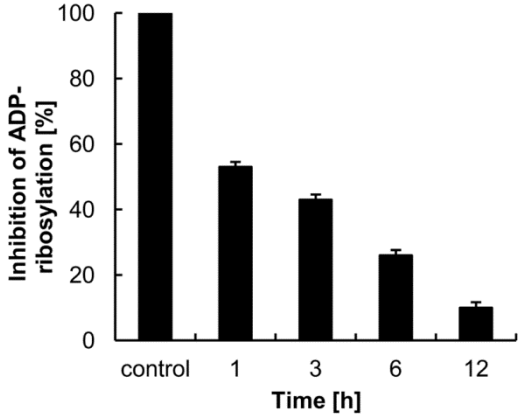

Fig. 1. Time-dependent decrease in intracellular enzymatic activity of FA. Cells (HUVEC) were treated as described in Materials and Methods. Cell lysates were prepared at the indicated times, and 10 μl aliquots were assayed for ADPrT activity in the presence of 20 pmol of rat liver eEF2. Cell lysates treated with diphtheria toxin were used to measure the enzymatic activity (FA~ 10 ng) for ADP-ribosylation of eEF2 (20 pmol).

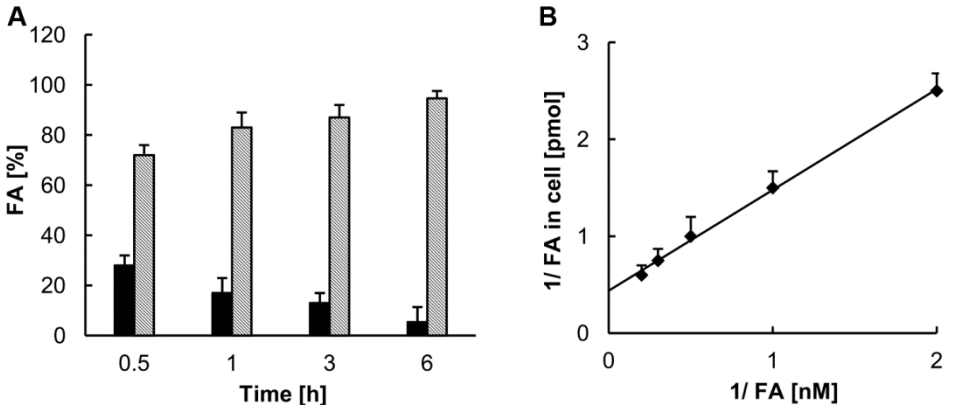

Fig. 2. Time course of DT uptake by HUVEC. A – Cells were incubated in the presence of 2 nM DT for the indicated time periods. The incubation conditions were as described in Materials and Methods. After incubation, the cells collected by centrifugation were lysed, and cell lysates were centrifuged for 5 min at 1500 x *g*. DT(FA) amounts in the pellet and supernatant fractions and in the cell culture medium were determined by ELISA. FA amounts in the cell culture medium (black bar) in the cell (striped bar) are shown. B – Dependence of uptake rate on DT concentration. Conditions were as in A, with incubation time adjusted to 10 min. The DT concentration varied between 0.5 and 5 nM. DT(FA) amounts in the cell were determined by ELISA, and data were plotted according to Lineweaver-Burk.

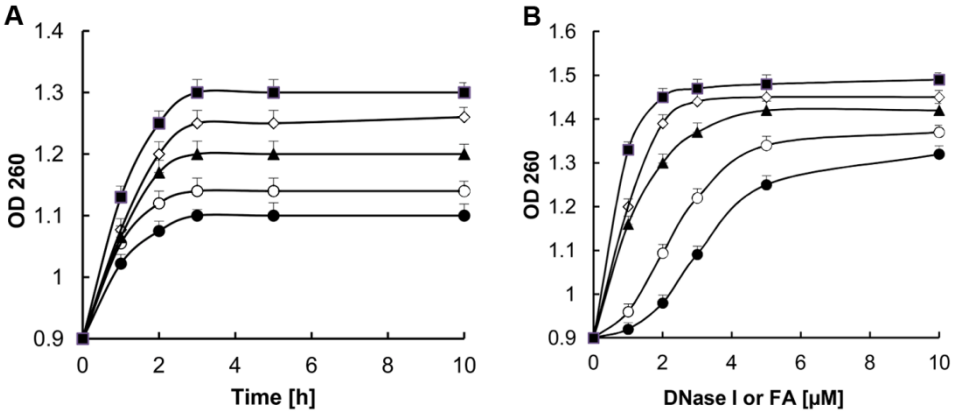

Fig. 3. Deoxyribonuclease activity of FA. A – Time-dependent changes in the hyperchromicity in DNA samples (80 μg/ml) were measured in the presence of FA (1.6 nmol), G-actin (70 μg) or DNase I (1.6 nmol). Experimental details were as described in Material and Methods. (■-■), with DNase I and FA; (◊-◊), with DNase I; (▲-▲), with FA, (○-○), DNase I and G-actin; (●-●) with FA and G-actin. B – Inhibition of deoxyribonuclease activity of FA and DNase I by G-actin. The incubation conditions were as in A, with the incubation time adjusted to 20 min and FA or DNase I amounts changed as indicated in the presence or absence of G-actin. (■-■), DNase I and FA; (◊-◊), with DNase I;(▲-▲), with FA; (○-○), with G-actin and DNase I; (●-●), with FA and G-actin.

Deoxyribonuclease activity

DT and FA have been repeatedly shown to possess deoxyribonuclease activity [23, 24]. These findings were confirmed in the present study as assayed by changes in hyperchromicity. FA exhibited a DNase activity that was comparable to DNase I (Fig. 3A). G-actin appeared to inhibit this activity. However, increasing amounts of FA or DNase I in the presence of a constant, limited amount of G-actin resulted in sigmoidal curves of hyperchromicity with an inflection point that approximately corresponded to the equimolarity of G-actin (Fig. 3B).

FA effect on actin filaments

In the present study, we revealed the depolymerisation of the actin cytoskeleton in DT-treated HUVEC. The amount of F-actin eluting in the void volume was reduced by half after the same period of time. A set of experiments were performed to determine whether the interaction between FA and F-actin was biologically relevant (Tab. 1). In the presence of cycloheximide, which is a protein synthesis inhibitor, the amount of F-actin was decreased by 12% in the 18^{th} hour. This proportion was determined with cytochalasin D, C2 toxin, DT and CRM 197 as 80%, 73%, 60% and 56%, respectively. In DT and CRM197 treated cells, the amount of F-actin was decreased by 60% and 65%, respectively, in P120 fractions. F-actin was visualised with rhodamine-phalloidin by using a fluorescence microscopy technique (Fig. 4A-B-C). The depolymerisation increased beginning at the third hour of treatment, which was concurrent with the shrinkage of cell size (Fig. 4B-C). We also explored the intracellular distribution of FA by using immunofluorescence microscopy with the FA-specific monoclonal antibody 7F2 (Fig. 4D-E). A prominent increase in F-actin depolymerisation has been shown to be dependent on the concentrations of DT (Fig. 4F). At the end of the 12^{th} hour, in DT-treated cells similar to C2 toxin, decrease in stress fibres and focal adhesion and also cell rounding was observed (unpublished data). The F-actin and G-actin levels were calculated from the triton-soluble filamentous actin (P2 and S2, respectively) following differential centrifugation. In the presence of the agents cycloheximide, DT, CRM197 and C2 toxin, the fragmentation of actin was increased at the 18^{th} hour by approximately 10-15%, 55%, 50% and 75%, respectively (Fig. 5A). Also, fragmentation of 80% was observed in the presence of cytochalasin D. The F-actin content of cells was investigated by quantification of rhodamine-phalloidin labelling (Fig. 5B). Western blot analysis was performed by using an anti-actin antibody (Fig. 5C). The findings were concordant with the fluorescent images. The actin level in S_2 increased, while the level of P_2 was reduced.

Tab. 1. DT(FA) effect on F-actin in the cell. HUVEC were incubated in the presence of 0.8 nM DT, 0.8 nM CRM197, 100 ng/ml C2 toxin, 0.5 µg/ml cycloheximide and 2 µM cytochalasin D for the indicated time periods. Cells were lysed, and cell lysates were fractioned on a Sephadex 4B column. FA, FA(CRM197) and actin amounts in the void volume fractions (alternatively actin in post-microsomal pellet (P120)) were determined by ELISA after depolymerisation, as described in Materials and Methods.

Treatment	In void volume or P120* (F-actin%)			
	1 h	3 h	6 h	12 h
None	51 ± 2.3	47 ± 1.6	49 ± 3.1	48 ± 1.2
DT	45 ± 2.6	39 ± 3.1	30 ± 4.4	19 ± 4.2
CRM197	44 ± 2.1	40 ± 2.3	28 ± 1.6	21 ± 3.2
C2 toxin	37 ± 1.5	25 ± 2.8	18 ± 3.1	13 ± 2.0
Cytochalasin D	25 ± 4.2	18 ± 3.7	15 ± 1.8	10 ± 2.2
Cycloheximide	45 ± 1.6	43 ± 2.4	42 ± 2.9	42 ± 0.9
*DT	46 ± 4.1	34 ± 2.6	28 ± 2.9	17 ± 3.4
*CRM197	44 ± 1.9	35 ± 0.9	31 ± 3.7	21 ± 1.8

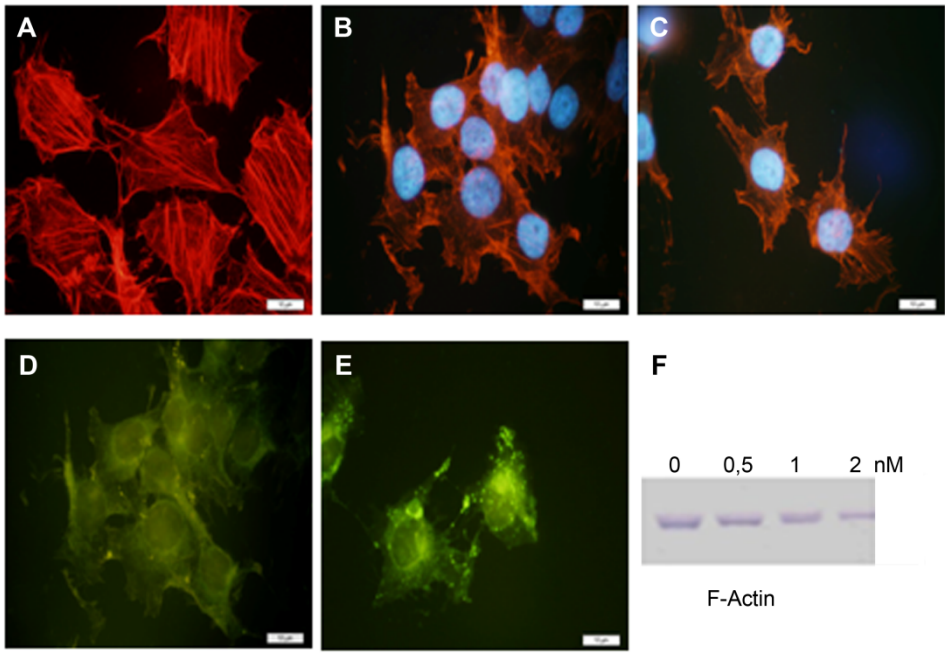

Fig. 4. Actin cytoskeleton treated with DT. HUVEC were incubated in the presence of 0.8 nM DT. A – Control, B – DT (3 h), C – DT (6 h). Actin filaments were visualised using rhodamine-phalloidin or Alexa 497-labelled (A, B, C) and nuclei in turn with DAPI (B, C). FA was detected using the murine monoclonal antibody 7F2 and FITC-labelled goat anti-mouse Ig antibody (D, E). The scale bar is 10 µm. F – Western blot analysis of F-actin with increasing amounts of DT treated cells during 6th hour. The amount of F-actin has been shown via G-actin/F-actin in vivo assay kit.

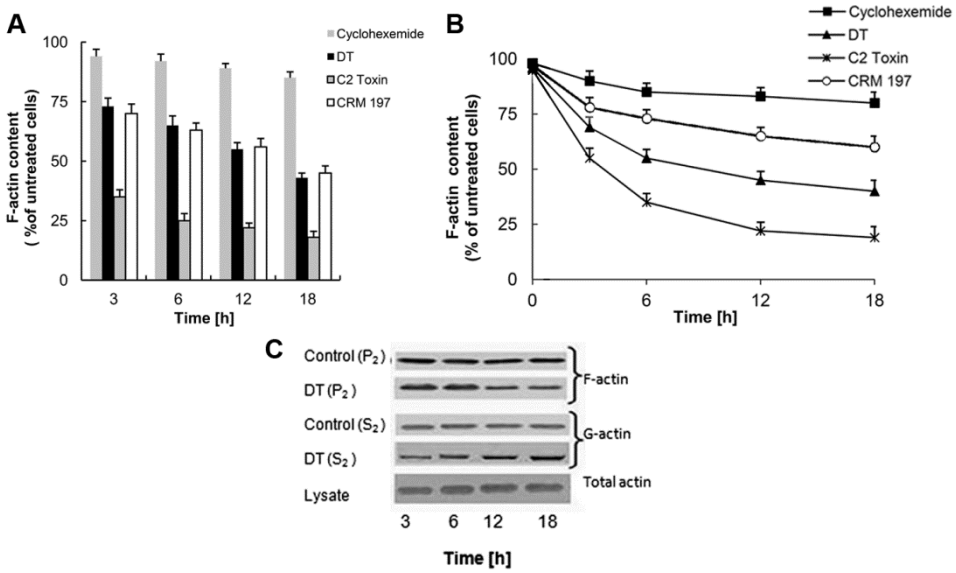

Fig. 5. Determination of intracellular F-actin in DT treated HUVEC. A – As explained in Materials and Methods, HUVEC were treated with 0.8 nM DT, 0.8 nM CRM197, 100 ng/ml C2 toxin and 0.5 µg/ml cycloheximide. Cell lysates were prepared at the indicated times. F-actin levels in the triton-soluble filamentous actin (P_2) were calculated using an anti-actin monoclonal antibody for ELISA, following depolymerisation. B – Rhodamine-phalloidin labelling of F-actin. (■-■), cycloheximide; (○-○), CRM197; (▲-▲), DT; (x-x), C2 toxin. C – Western blot analysis of cell lysates, P2 and S2 fractions (10 µg) was performed following SDS-PAGE, using an anti-actin antibody.

DISCUSSION

FA has been known for decades for its eEF2-specific ADPrT activity. The inhibition of protein synthesis is regarded to be the sole cause of FA cytotoxicity [25, 26]. Nevertheless, the existence of cell lines that do not undergo cell death due to FA-mediated inhibition of protein synthesis [27] raises the question of the causal relationship between these events. Besides the inhibition of protein synthesis, DT results in the breakdown of the cytoskeleton, internucleosomal DNA cleavage and cytolysis. A deoxyribonuclease activity inherent to FA has also been reported. These events follow the onset of the inhibition of protein synthesis by a lag of several hours and correspond to those events associated with programmed cell death type I [28]. Inhibition of the protein synthesis is consistent with the report that in the same cell line, i.e., Vero cells, the presence of DT even in high concentrations could not induce cytolysis or DNA fragmentation even though these cells are highly sensitive to protein synthesis inhibition by DT [29].

The results of our previous study indicate that FA can interact with both G- and F-actin. The binding to the latter appears to take place at the plus end of the filament, blocking its further polymerisation [13]. In the endocytic process, the

cargo role of actin has been identified. However, the eEF2-actin interaction was previously reported [16]. In our recent studies, we showed that eEF2 played a role in intracellular trafficking of FA and its release from early endosomes to the cytosol [14]. These results, which reveal a previously unknown feature of the action of FA, may provide further insight into the mechanism of the cytotoxicity of DT. The relationship between the reported FA-actin interaction and cell toxicity requires elucidation. Recent findings showed that actin can inhibit the FA-mediated ADP-ribosylation of eEF2 [12]. The present investigation provides a possible explanation for this inhibition, suggesting that actin-bound FA may be unable to promote this reaction. However, an abundance of actin molecules challenged the effectiveness of FA in depolymerising actin filaments in the cell.

Our results indicate that the diphtheria toxin-dependent inhibition of protein synthesis is followed by a time-dependent inactivation of FA in the post-microsomal supernatant (S120), the association of FA with an actin-containing protein complex, and the breakdown of the actin cytoskeleton. The effect of FA on actin filaments does not appear to have a connection to its ADPrT activity because benzamidine-treated DT and non-toxic DT (CRM197) appear to bind to F-actin both *in vitro* and *in vivo*. Moreover, DT (CRM197) binding also gives rise to F-actin breakdown, which underlines the cytotoxic effect of CRM197.

The severing effect of FA on F-actin filaments may be reduced significantly by the cellular abundance of actin molecules. The actin concentration in the cell is estimated to vary from 50 to 100 μM, with nearly half of actin molecules being arranged as F-actin filaments. Each filament contains an average of ten or more actin monomers [30]. Therefore, the cellular concentration of plus ends should be in the range of 1-5 μM. A toxin concentration of around 1 nM in the culture medium has been found sufficient for cell death and, unless otherwise indicated, was used throughout this study. However, DT uptake by the cells is in line with previous reports [31, 32]; the uptake is very efficient and was nearly complete in the course of the first few hours of incubation. The internalisation thus gives rise to elevation of intracellular DT(FA) concentration by several orders of magnitude over the initial toxin concentration in the culture medium. Consequently, with its cellular concentration reaching levels in the range of the Kd value of the interaction, FA is likely enabled to block the plus ends.

The actin cytoskeleton is known to be the target of several bacterial proteins [33]. Some of these, i.e., clostridial binary toxins, give rise to the degradation of actin filaments by ADP-ribosylation of actin monomers [34, 35]. Other toxins from the clostridial family inactivate *Rho* proteins by glycosylation, while cytotoxic necrotic factors from *E. coli* utilise deamination [30]. Other factors with protease activity promote the reorganisation of the actin skeleton. The reported interaction of FA with actin appears to add a new dimension to this complex picture. Bacterial toxins with the ability to interact with actin deserve consideration, especially in light of the prokaryotic origins of the actin cytoskeleton [36].

Acknowledgements. This work was supported by the Scientific and Technological Research Council of Turkey [TÜBİTAK] (Grant No. 107S032) and in part by the Research Fund of İstanbul University (Grant No. 463-04012006).

REFERENCES

1. Collier, R.J. Understanding the mode of action of diphtheria toxin: a perspective on progress during the 20th century. **Toxicon** 39 (2001) 1793-1803.
2. Choe, S., Bennett, M.J., Fujii, G., Curmi, P.M., Kantardjieff, K.A., Collier, R.J. and Eisenberg, D. The crystal structure of diphtheria toxin. **Nature** 357 (1994) 216-222.
3. Kageyama, T., Ohishi, M., Miyamoto, S., Mizushima, H., Iwamoto, R. and Mekada, E. Diphtheria toxin mutant CRM197 possesses weak EF2-ADP-ribosyl activity that potentiates its anti-tumorigenic activity. **J. Biochem.** 142 (2007) 95-104.
4. Rönnberg, B.J. and Middlebrook, J.L. Cellular regulation of diphtheria toxin cell surface receptors. **Toxicon** 27 (1989) 1377-1388.
5. Van Ness, B.G., Howard, J.B. and Bodley, J.W. ADP-ribosylation of elongation factor 2 by diphtheria toxin. NMR spectra and proposed structures of ribosyl-diphthamide and its hydrolysis products. **J. Biochem.** 255 (1980) 10710-10716.
6. Collier, R.J. Effect of diphtheria toxin on protein synthesis: inactivation of one of the transfer factors. **J. Mol. Biol.** 25 (1967) 83-98.
7. Draper, R.K. and Simon, M.I. The entry of diphtheria toxin into the mammalian cell cytoplasm: evidence for lysosomal involvement. **J. Cell Biol.** 87 (1980) 849-854.
8. Kaul, P., Silverman, J., Shen, W. H., Blanke, S.R., Huynh, P.D., Finkelstein, A. and Collier, J. Roles of Glu 349 and Asp 352 in membrane insertion and translocation by diphtheria toxin. **Protein Sci.** 5 (1996) 687-697.
9. D'Silva, P.R. and Lala, A.K. Organisation of diphtheria toxin in membranes. A hydrophobic photolabeling study. **J. Biol. Chem.** 275 (1998) 11771-11777.
10. Lemichez, E., Bomsel, M., Devilliers, G., Vander Spek, J., Murphy, J.R., Lukianov, E.V., Olsnes, S. and Bouquet, P. Membrane translocation of diphtheria toxin fragment A exploits early to late endosome trafficking machinery. **Mol. Microbiol.** 23 (1997) 445-457.
11. Burch, G.E., Sun, S.C., Sohal, R.S., Chu, K.C and Colcolough, H.L. Diphtheritic myocarditis. A histochemical and electron microscopic study. **Am. J. Cardiol.** 21 (1968) 261-268.
12. Bektaş, M., Günçer, B., Güven, C., Nurten, R. and Bermek, E. Actin-an inhibitor of eukaryotic elongation factor activities. **Biochem. Biophys. Res. Commun.** 317 (2004) 1061-1066.
13. Bektaş, M., Varol, B., Nurten, R. and Bermek, E. Interaction of diphtheria toxin (fragment A) with actin. **Cell Biochem. Funct.** 27 (2009) 430-439.

14. Bektaş, M., Hacıosmanoğlu, E., Özerman, B., Varol, B., Nurten, R. and Bermek, E. The effect of cytochalasin D and the involvement of actin filaments and eukaryotic elongation factor 2 in the release of diphtheria toxin fragment a into the cytosol. **Int. J. Biochem. Cell Biol.** 43 (2011) 1365-1372.
15. Bektaş, M., Nurten, R., Ergen, K. and Bermek, E. Endogenous ADP-ribosylation for eukaryotic elongation factor 2: evidence of two different sites and reactions. **Cell Biochem. Funct.** 24 (2006) 369-380.
16. Bektaş., M., Nurten., R., Gürel., Z., Sayers, Z. and Bermek, E. Interactions of eukaryotic elongation factor 2 with actin: a possible link between protein synthetic machinery and cytoskeleton. **FEBS Lett.** 356 (1994) 89-93.
17. Bektaş, M., Nurten, R., Sayers, Z. and Bermek, E. Interactions of eukaryotic elongation factor 2 with the cytoskeleton interference with DNase I binding to actin. **Eur. J. Biochem.** 256 (1998) 142-147.
18. Engvall, E. Enzyme immunoassay ELISA and EMIT. **Meth. Enzymol.** 70 (1980) 419-439.
19. Laemmli, U.K. Cleavage of structural proteins during the assembly of the head of bacteriophage T4. **Nature** 227 (1970) 680-685.
20. Dharmawardhane, S., Warren, V., Hall, A.L. and Condeelis, J. Changes in the assosication of actin binding proteins with the actin cytoskeleton during chemotactic stimulation of *Dictiyostelium discoideum*. **Cell Motil. Cytoskeleton** 13 (1989) 57-63.
21. Tu, Y., Wu, S., Shi, X., Chen, K. and Wu, C. Migfilin and Mig-2 ling focal adhesions to filamin and the actin cytoskeleton and function in cell shape modulation. **Cell** 113 (2003) 37-47.
22. Gibert, M., Marvaud, J.C., Pereira, Y., Hale, M.L., Stiles, B.G., Boquet, P., Lamaze, C. and Popoff. M.R. Differential requirement for the translocation of clostridial binary toxins: Iota toxin requires a membrane potential gradient. **FEBS Lett.** 581 (2007) 1287-1296.
23. Bruce, C., Baldvin, R.L., Lessnik, S.L. and Wisnieski, B.J. Diphtheria toxin and its ADP-ribosyltransferase-defective homologue CRM197 possess deoxyribonuclease activity. **Proc. Natl. Acad. Sci**. **USA** 87 (1990) 2995-2998.
24. Lessnick, S.L., Lyczak, J.B., Bruce, C., Lewis, D.G., Kim, P.S., Stolowitz, M.L., Hood, L. and Wisnieski, B.J. Localization of diphtheria toxin nuclease activity to fragment A. **J. Bact.** 174 (1992) 2032-2038.
25. Pappenheimer, A.M. Jr. and Gill, D.M. Diphtheria. **Science** 26 (1973) 353-358.
26. Collier, R.J. Diphtheria toxin: mode of action and structure. **Bacteriol. Rev.** 39 (1975) 54-85.
27. Morris, R.E. and Saelinger, C.E. Diphtheria toxin does not enter resistant cells by receptor-mediated endocytosis. **Infect. Immun.** 42 (1987) 812-817.
28. Bras, M., Queenan, B. and Susin, A. Programmed cell death via mitochondria: different modes of dying. **Biochemistry (Mosc.)** 70 (2005) 231-233.
29. Kusano, I., Kageyama, A., Tamura, T., Oda, T. and Muramatsu, T. Enhancement of diphtheria toxin-induced apoptosis in Vero cells by

combination treatment with brefeldin A and okadaic acid. **Cell Struct. Funct.** 26 (2001) 279-288.
30. Barth, H., Olenik, C., Sehr, P., Schmidt, G., Aktories, K. and Mayer, D.K. Neosynthesis and activation of Rho by *Escherichia coli* cytotoxic necrotizing factor (CNF1) reverse cytopathic effects of ADP-ribosylated Rho. **J. Biol. Chem.** 274 (1999) 27407-27414.
31. Cha, J.H., Brook, J.S., Ivey, K.N. and Eidels, L. Cell surface monkey CD9 antigen is a coreceptor that increases diphtheria toxin sensitivity and diphtheria toxin receptor affinity. **J. Biol Chem.** 275 (2000) 6901-6907.
32. Brooke, J.S., Cha, J.H. and Eidels, L. Diphtheria toxin receptor interaction: association, dissociation, and effect of pH. **Biochem. Biophys. Res. Commun.** 248 (1998) 297-302.
33. Richard, J.F., Petit, L., Gibert, M., Marvaud, J.C., Bouchaud, C. and Popoff, M. Bacterial toxins modifying the actin cytoskeleton. **Internal. Microbiol.** 2 (1999) 185-194.
34. Aktories, K. and Wegner, A. ADP-ribosylation of actin by clostridial toxins. **J. Cell. Biol.** 109 (1989) 1385-1387.
35. Aktories K., Barmann, M., Ohishi, I., Tsuyama, S., Jakobs, K.H. and Haberman, E. Botulinum C2 toxin ADP-ribosylates actin. **Nature** 322 (1986) 390-392.
36. Van den Ent, F., Amos, L.A. and Löwe, J. Prokaryotic origin of the actin cytoskeleton. **Nature** 413 (2001) 39-44.